A Practical Criterion for Screening Stable Boron Nanostructures

Supporting Information

Shao-Gang Xu[†,‡], Yu-Jun Zhao[†], Xiao-Bao Yang[*†,‡], and Hu Xu[*‡]

[†]Department of Physics, South China University of Technology, Guangzhou 510640, P. R. China

[‡]Department of Physics, South University of Science and Technology of China, Shenzhen 518055, P. R. China

Equivalent judgment for possible candidates

According to our constraints, the N-ring(N≥4) tubular structures should be introduced a few vacancies. While, how to form the tubular clusters with vacancies? We design the hexagonal vacancies at the internal layers of the intact rings. Simply, we create a few hexagonal vacancies in the same layer of the structures. If add one vacancy, we will get only one kind of the equivalent structure, as all the atoms on the certain circle occupy the degenerate positions. However, based on the congruence check, if we add two or more vacancies at the same layer, we must consider the equivalent judgement to eliminate the degenerate structures. In the Figure S1, we suppose that there are n atoms in the same layer, the bigger size atoms represent vacancies of the structures. First, we move the structure to ensure the center of the system locate at (0,0,0). As there are n atoms in the same layer, and if you rotate clockwise the structure (b) n times you can get n equivalent structures. For example, rotating the structure (b) $(\frac{4\pi}{n})$ degrees, and we can get the structure (a). So the rotation operation was involved to eliminate the degenerate structures. On the other hand, there exist a few space configurations are symmetrical with respect to the center point or a plan. In the Figure S1, structure (b) and (c) are symmetrical respect to the center point. In order to eliminate these symmetrical chiral structures, based on one of the symmetrical structures (c), and we introduce rotation operations n times for the (c) to screen other equivalent chiral structures and their mirror structures. Actually, we adopt rotation operations $4n$ times for initial structure to eliminate other degenerate structures.

---

[*] E-mail address: scxbyang@scut.edu.cn
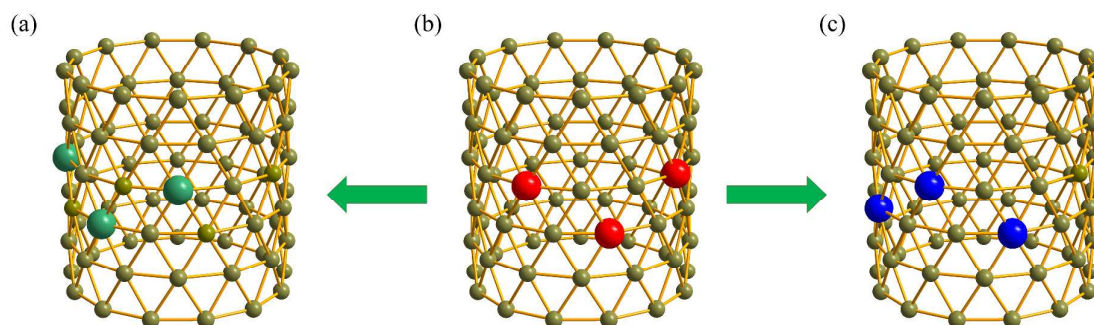[*] E-mail address: xu.h@sustc.edu.cn

Figure S1. Initial structures of the B tubular cluster. The green dot, red dot and blue dot in a, b and c represent the hexagonal vacancies of the corresponding structures.
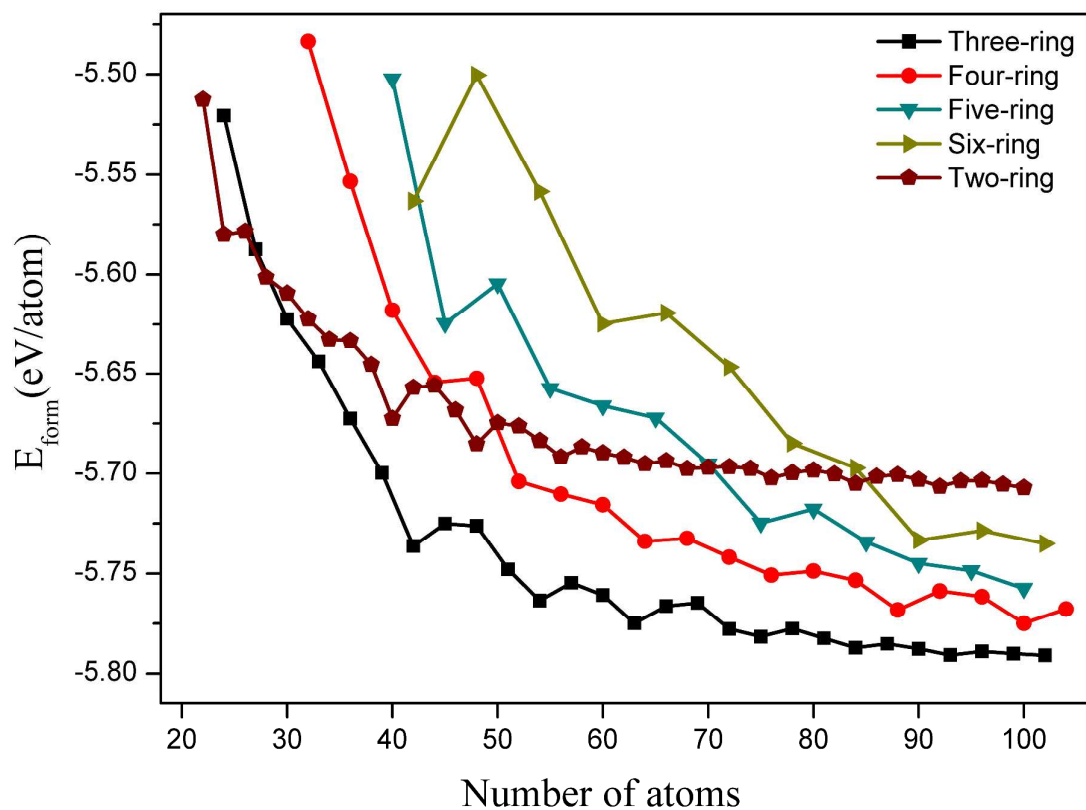

Figure S2. Relation of average formation energy (E_{form}) and size of the N-ring tubular B_n clusters. The E_{form} of   N-ring(N=2~6) tubular clusters represent as solid pentagons, solid squares, solid dots and solid triangles, respectively.
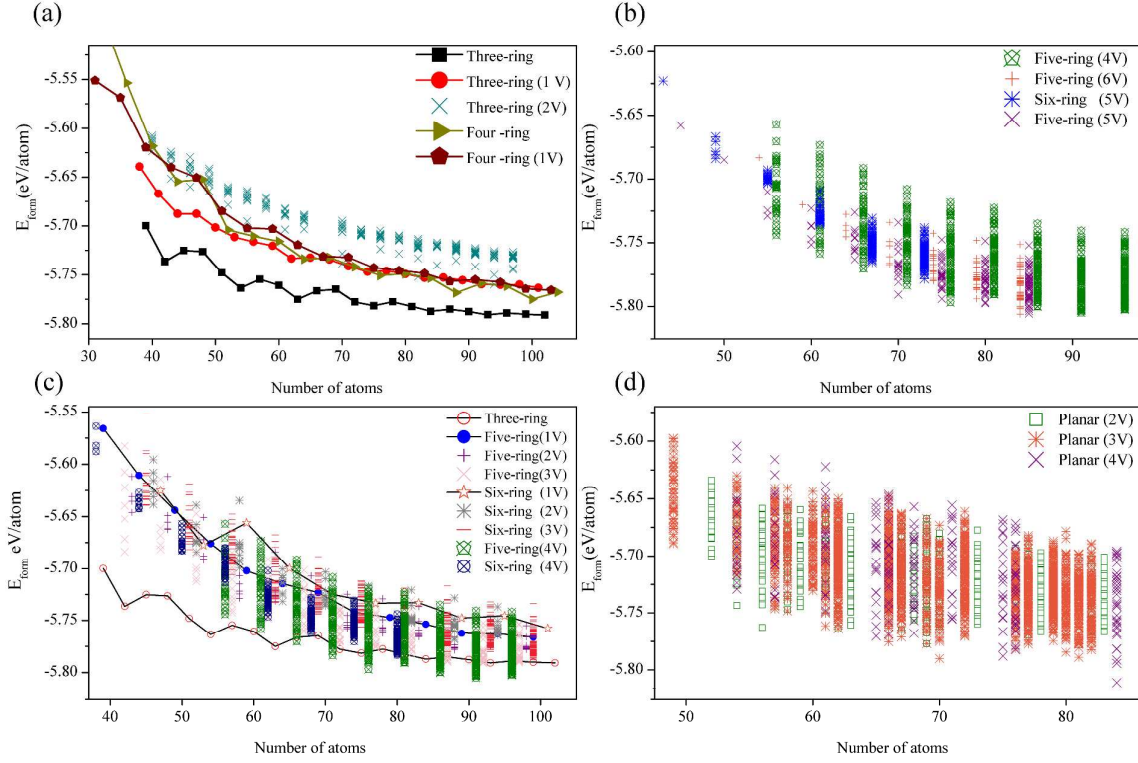
Figure S3. Relation of average formation energy(E_{form}) and the size of the cluster. (a-c) The different symbols represent N-ring tubular B_n clusters with various hexagonal vacancies. The detail of the symbols shown in the legends. (d) The different symbols represent the quasi-planar B_n clusters with various hexagonal vacancies. (V represents hexagonal vacancy)
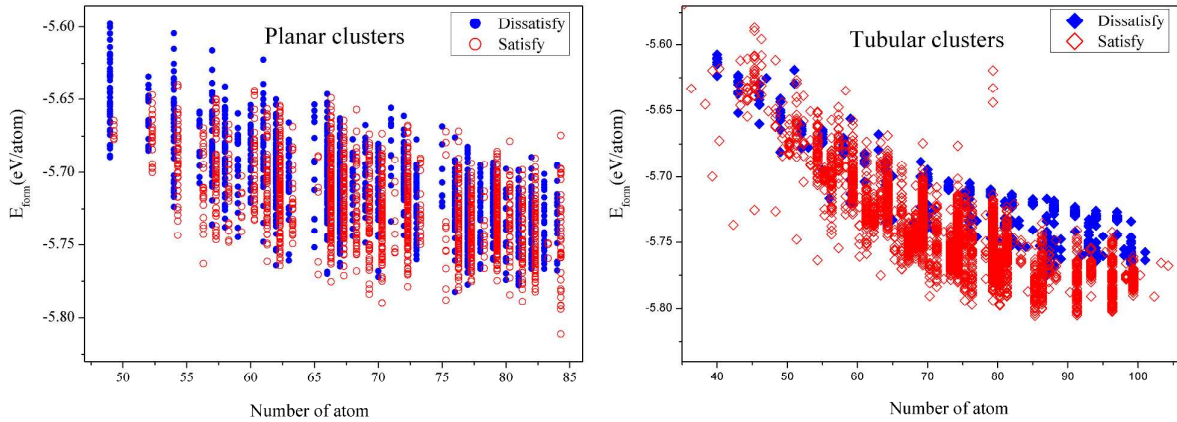
Figure S4. The results of the 8-electron model solutions for all the B_n (n=50~85) planar and tubular clusters. (a) The empty dots represent there exist a solution for the model, the solid dots represent there doesn't exist a solution for the model. (b) The empty diamonds represent there exist a solution for the model, the solid diamonds represent there doesn't exist a solution for the model.

Figure S5. The average formation energy (E_{form}) and structures of the stable quasi-planar and tubular(M layer N vacancies[M l N v]) B_n (n=50~84)clusters.
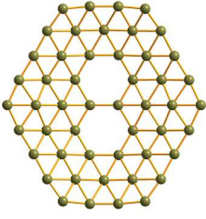
Quasi-planar structure   Tubular structure   Quasi-planar structure   Tubular structure

B$_{50}$ E$_{form}$(-5.720eV)   B$_{50}$ E$_{form}$(-5.683eV)[6 l 4 v]   B$_{51}$ E$_{form}$(-5.710eV)   B$_{51}$ E$_{form}$(-5.748eV) [3 l]
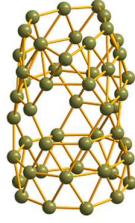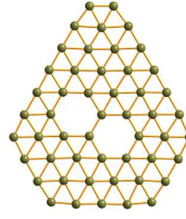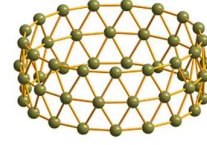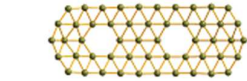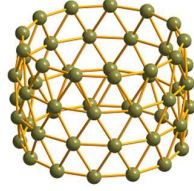
B$_{52}$ E$_{form}$(-5.700eV)   B$_{52}$ E$_{form}$(-5.704eV) [4 l]   B$_{53}$ E$_{form}$(-5.691eV) [5 l 2 v]
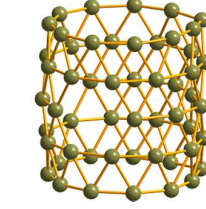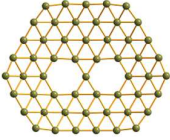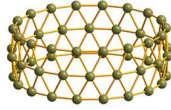
B$_{54}$ E$_{form}$(-5.744eV)   B$_{54}$ E$_{form}$(-5.764eV) [3 l]   B$_{55}$ E$_{form}$(-5.729eV) [5 l 5 v]
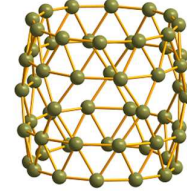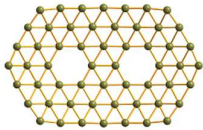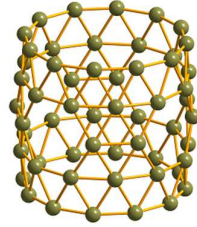
B$_{56}$ E$_{form}$(-5.763eV)   B$_{56}$ E$_{form}$(-5.744eV) [5 l 4 v]   B$_{57}$ E$_{form}$(-5.746eV)   B$_{57}$ E$_{form}$(-5.755eV) [3 l]
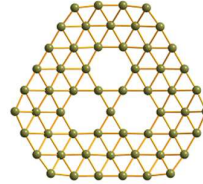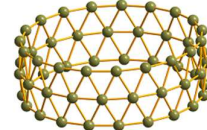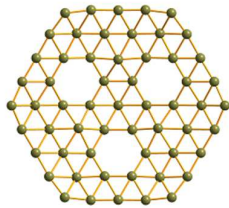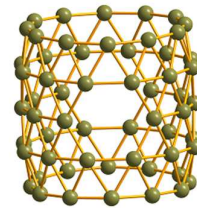
B$_{58}$ E$_{form}$(-5.748eV)   B$_{58}$ E$_{form}$(-5.728) [5 l 2 v]   B$_{59}$ E$_{form}$(-5.745eV)   B$_{59}$ E$_{form}$(-5.728eV) [5 l 6 v]
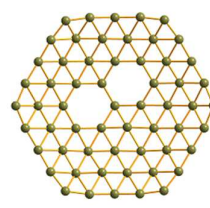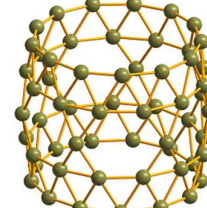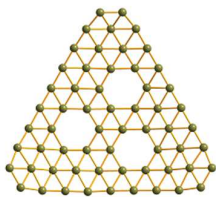
B$_{60}$ E$_{form}$(-5.733eV)
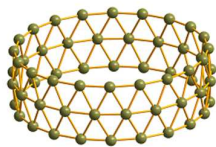
B$_{60}$ E$_{form}$(-5.761eV) [3 l]
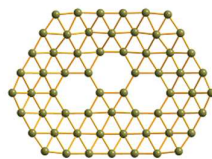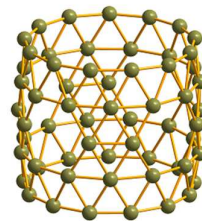
B$_{61}$ E$_{form}$(-5.762eV)

B$_{61}$ E$_{form}$(-5.759eV) [5 l 4 v]
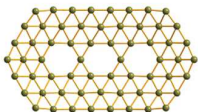
B$_{62}$ E$_{form}$(-5.764eV)
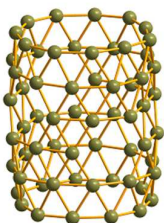
B$_{62}$ E$_{form}$(-5.747eV) [6 l 4 v]
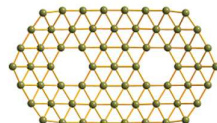
B$_{63}$ E$_{form}$(-5.761eV)
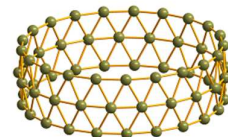
B$_{63}$ E$_{form}$(-5.775eV) [3 l]
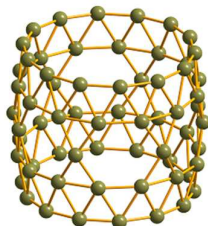
B$_{64}$ E$_{form}$(-5.745eV) [5 l 6 v]
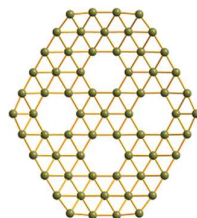
B$_{65}$ E$_{form}$(-5.770eV)
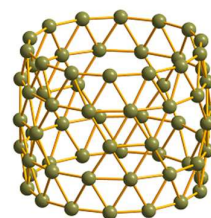
B$_{65}$ E$_{form}$(-5.763eV) [5 l 5 v]
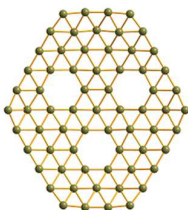
B$_{66}$ E$_{form}$(-5.775eV)
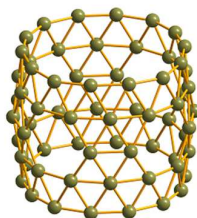
B$_{66}$ E$_{form}$(-5.770eV) [5 l 4 v]
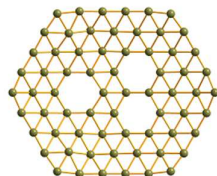
B$_{67}$ E$_{form}$(-5.771eV)
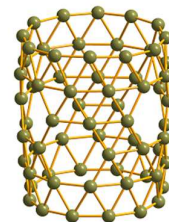
B$_{67}$ E$_{form}$(-5.766eV) [6 l 5 v]
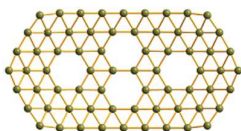
B$_{68}$ E$_{form}$(-5.768eV)
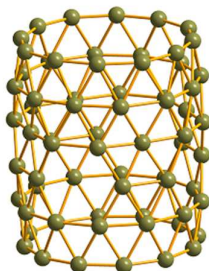
B$_{68}$ E$_{form}$(-5.762eV) [6 l 4 v]
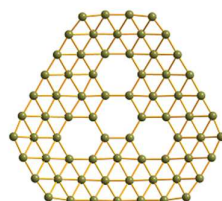
B$_{69}$ E$_{form}$(-5.784eV)
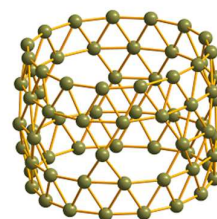
B$_{69}$ E$_{form}$(-5.767eV) [5 l 6 v]
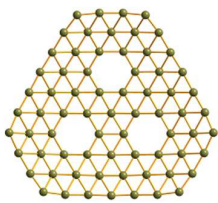
B$_{70}$ E$_{form}$(-5.790eV)
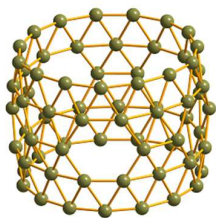
B$_{70}$ E$_{form}$(-5.791eV) [5 l 5 v]
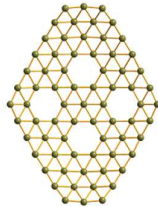
B$_{71}$ E$_{form}$(-5.756eV)
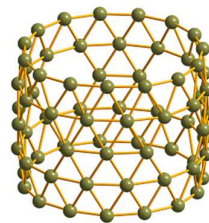
B$_{71}$ E$_{form}$(-5.784eV) [5 l 4 v]
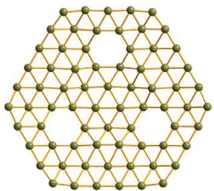
B$_{72}$ E$_{form}$(-5.779eV)
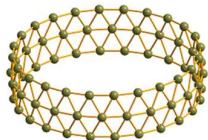
B$_{72}$ E$_{form}$(-5.778eV) [2 l]
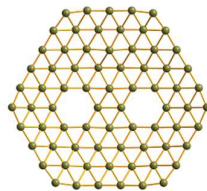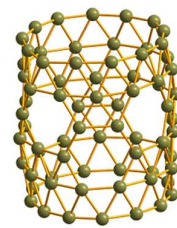
B$_{73}$ E$_{form}$(-5.760eV)

B$_{73}$ E$_{form}$(-5.778eV) [6 l 5 v]
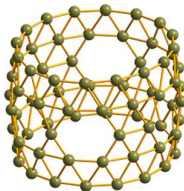
B$_{74}$ E$_{form}$(-5.780eV) [5 l 6 v]
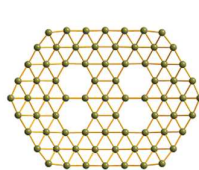
B$_{75}$ E$_{form}$(-5.788eV)
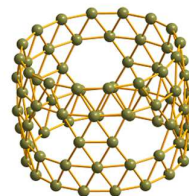
B$_{75}$ E$_{form}$(-5.794eV) [5 l 5 v]
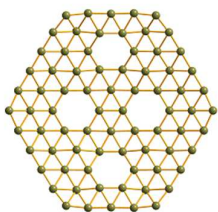
B$_{76}$ E$_{form}$(-5.782eV)
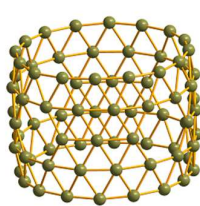
B$_{76}$ E$_{form}$(-5.797eV) [5 l 4 v]
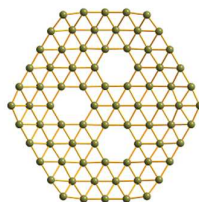
B$_{77}$ E$_{form}$(-5.777eV)
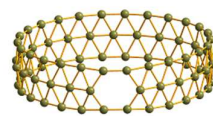
B$_{77}$ E$_{form}$(-5.746eV) [3 l 1 v]
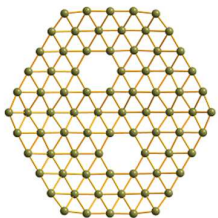
B$_{78}$ E$_{form}$(-5.767eV)
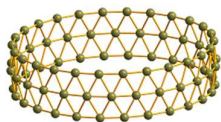
B$_{78}$ E$_{form}$(-5.778) [3 l]
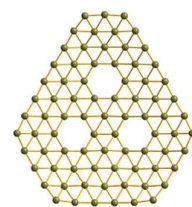
B$_{79}$ E$_{form}$(-5.775eV)

B$_{79}$ E$_{form}$(-5.794eV) [5 l 6 v]

B_{80} E_{form}(-5.784eV)

B_{80} E_{form}(-5.798eV) [5 1 5 v]

B_{81} E_{form}(-5.789eV)

B_{81} E_{form}(-5.791eV) [5 1 4 v]

B_{82} E_{form}(-5.782eV)

B_{82} E_{form}(-5.752eV) [6 1 2 v]

B_{83} E_{form}(-5.767eV)

B_{83} E_{form}(-5.766eV) [5 1 2 v]

B_{84} E_{form}(-5.811eV)
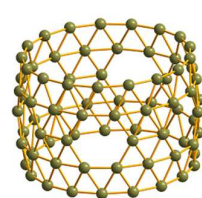
B_{84} E_{form}(-5.787eV) [5 1 6 v]
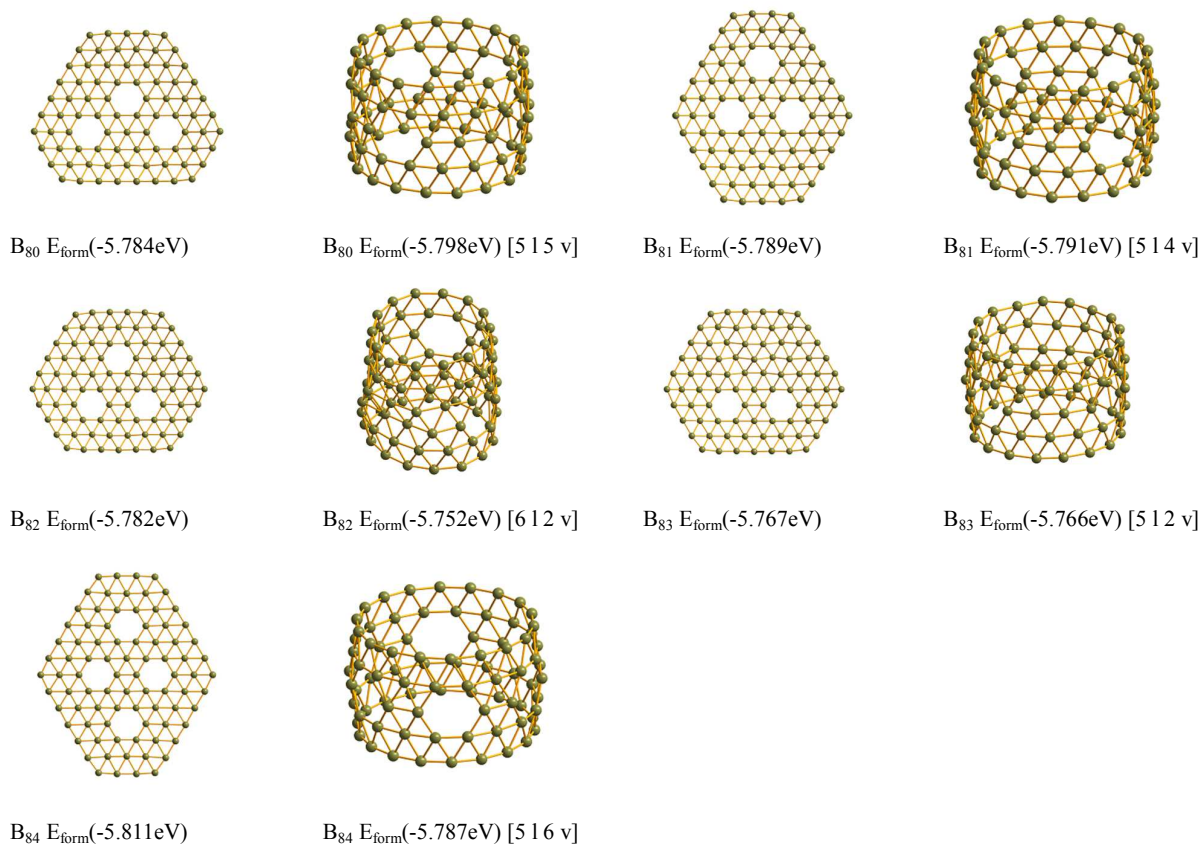
Table S1

B_n clusters	VASP(H-L) gap(eV)	$Dmol^3$(H-L) gap(eV)	HSE06(H-L) gap(eV)
B_{20} tubular	1.358	1.391	2.012
B_{42} tubular	1.365	1.313	1.564
B_{80} cage	1.013	1.157	1.425
B_{70} tubular	0.834	0.863	1.016
B_{76} tubular	0.870	0.924	1.169
B_{84} planar	0.422	0.446	0.575

Figure S6. The B$_n$ tubular clusters and the corresponding B nanoribbon. (a)The structure of the B$_{70}$ tubular cluster. (b) The nanoribbon based on unit of 14 atoms. (c) The structure of the B$_{76}$ tubular cluster. (d) The nanoribbon based on unit of 19 atoms.

Figure S7. Bond analysis for the stable B_{20}, B_{42} cluster: (a,b-1) the structure of B_{20}, B_{42} (a,b-2) isosurface of charge di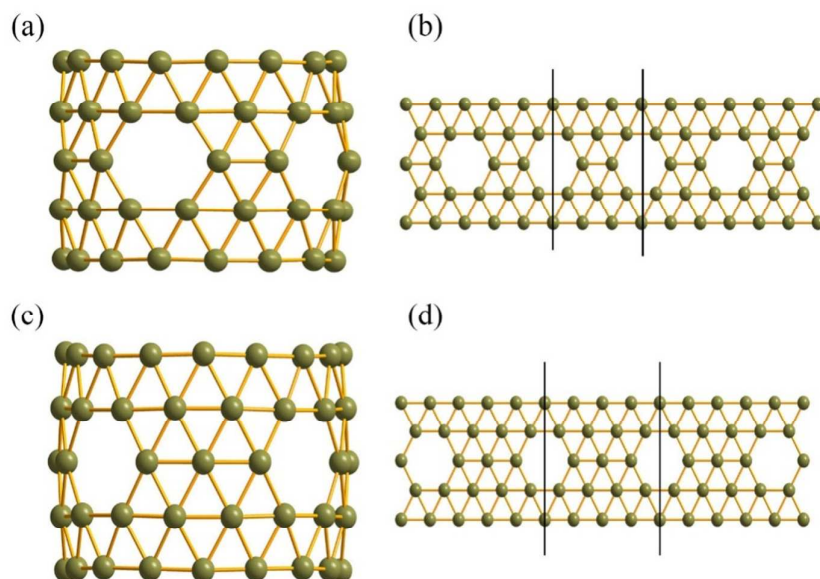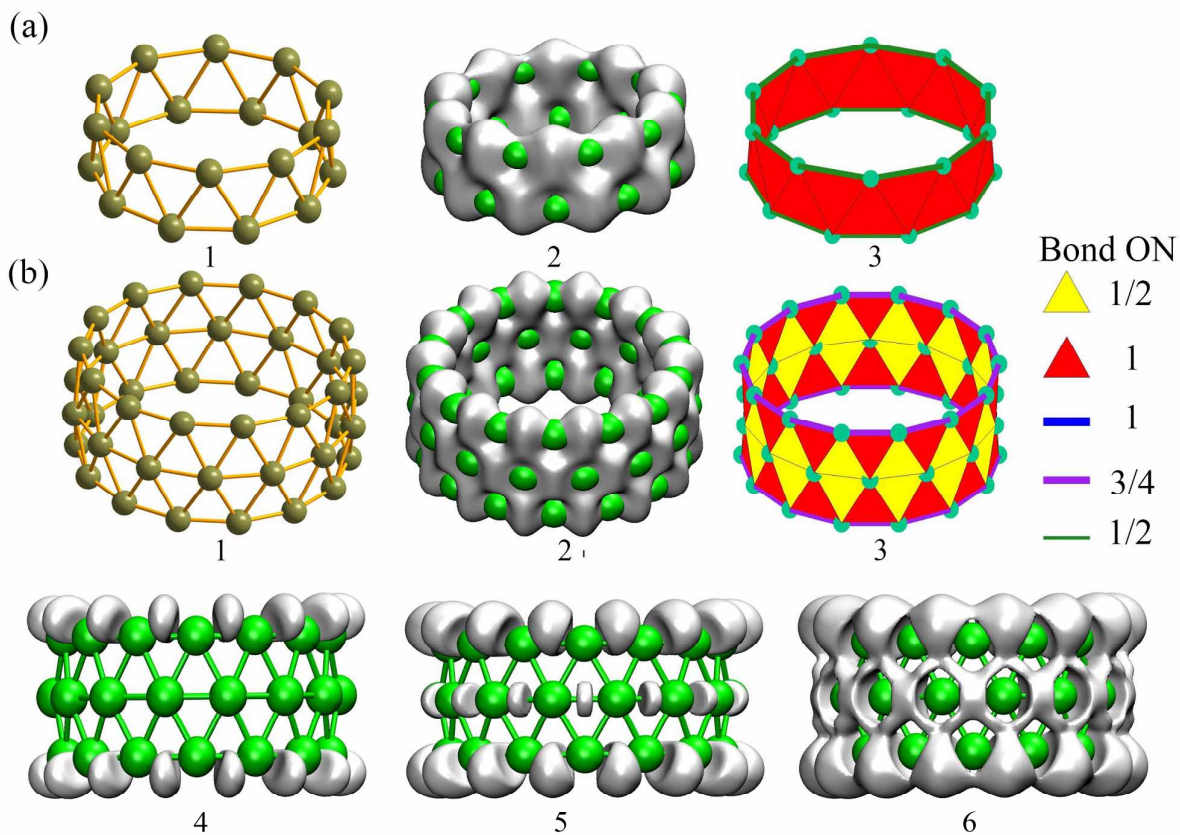fference for B_{20}, B_{42} (a,b-3) the distribution of 2c-2e and 3c-2e bonds. The occupation number for the 2c-2e and 3c-2e bonds are listed on the right side. (b-4~6) The Electron Localization Function(ELF) at values of 0.83, 0.75 and 0.68 for the B_{42} cluster.

The stable quasi-planar B_{56}, B_{70} clusters, all of them can be explained through our bond model. B_{56} belong to the symmetry group of C_{2v}, the bonds distribution is shown in the Figure S8b, which is agreed with charge difference. Insight in the charge difference, we found the electrons are localized at the convex point of the profiles. The B_{70} cluster is a highly symmetrical structure (C_{3v}), in order to guarantee our bond model meets the actual charge difference, we introduce the occupation number of 1/6, and figure out a new bonds distribution shown in the Figure S8d. This solution shares the same symmetry group as the charge difference(c). Insight the ELF isosurface map of all the quasi-planar B_n clusters in the Figure S9, which can also verify the result from our bond model analysis. For the stable B_{70} tubular cluster, the bond distribution contains 50(10) bonds 3c–2e(2c–2e) with the occupations of 1, and 40(50) bonds of 3c–2e(2c–2e) with the occupations of 1/2, as shown in the Figure S10-6.
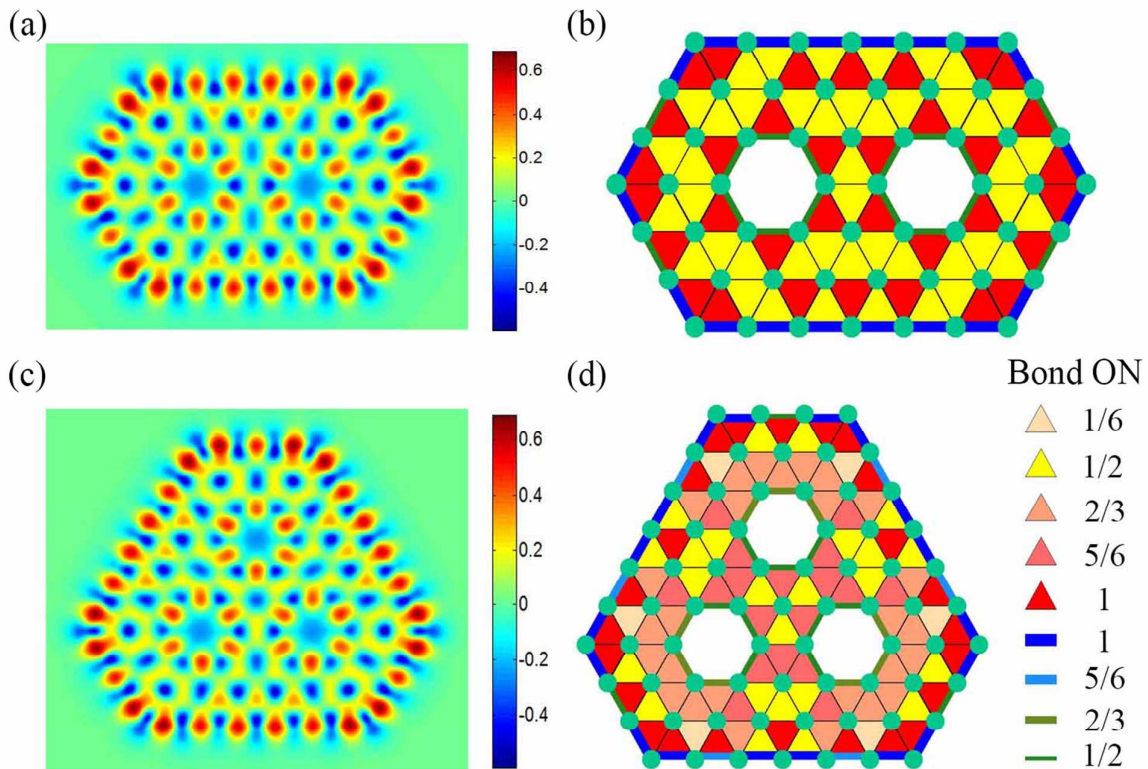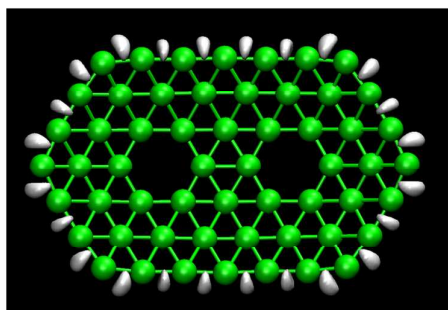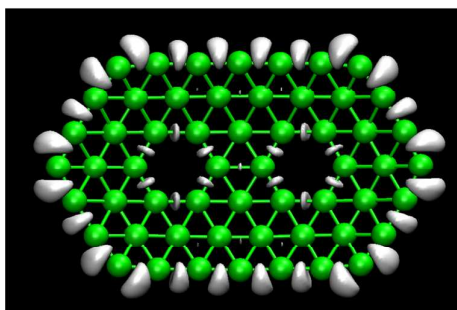

Figure S8. Bonding analysis for the stable B_{56}, B_{70}. (a,c) are the charge difference of coresponding structures. (b,d) possible distributions of 2c–2e and 3c–2e bonds. The corresponding distribution of 2c-2e and 3c-2e bonds with various occupation number are list on the right side.
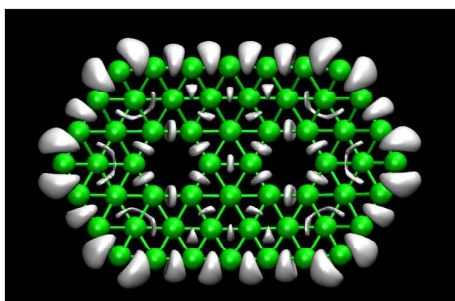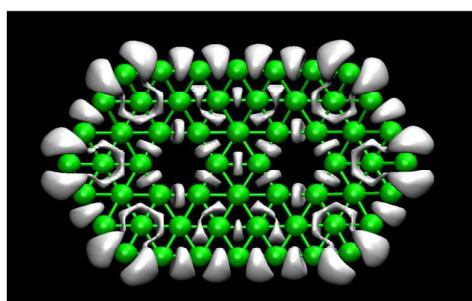
(a)
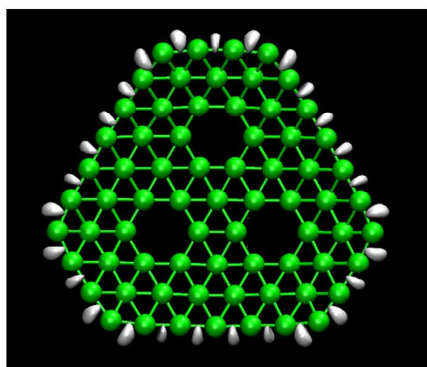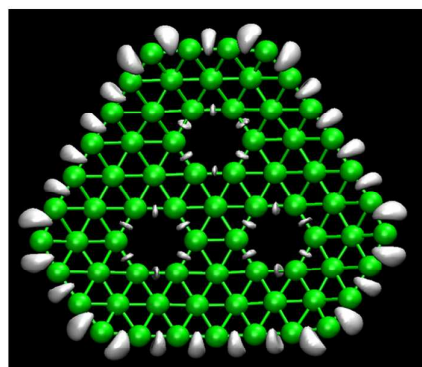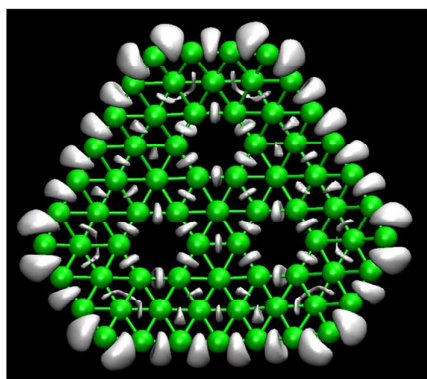

1

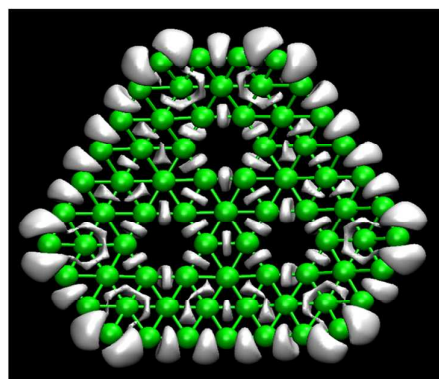
2

3

4

(b)

1

2

3

4

Figure S9. The Electron Localization Function(ELF) at various values of planar B_{56}, B_{70} clusters. The iso-values of (a-1~4) are 0.93, 0.85, 0.80 and 0.77, respectively. The iso-values of (b-1~4) are 0.92, 0.86 , 0.80 and 0.76, respectively.
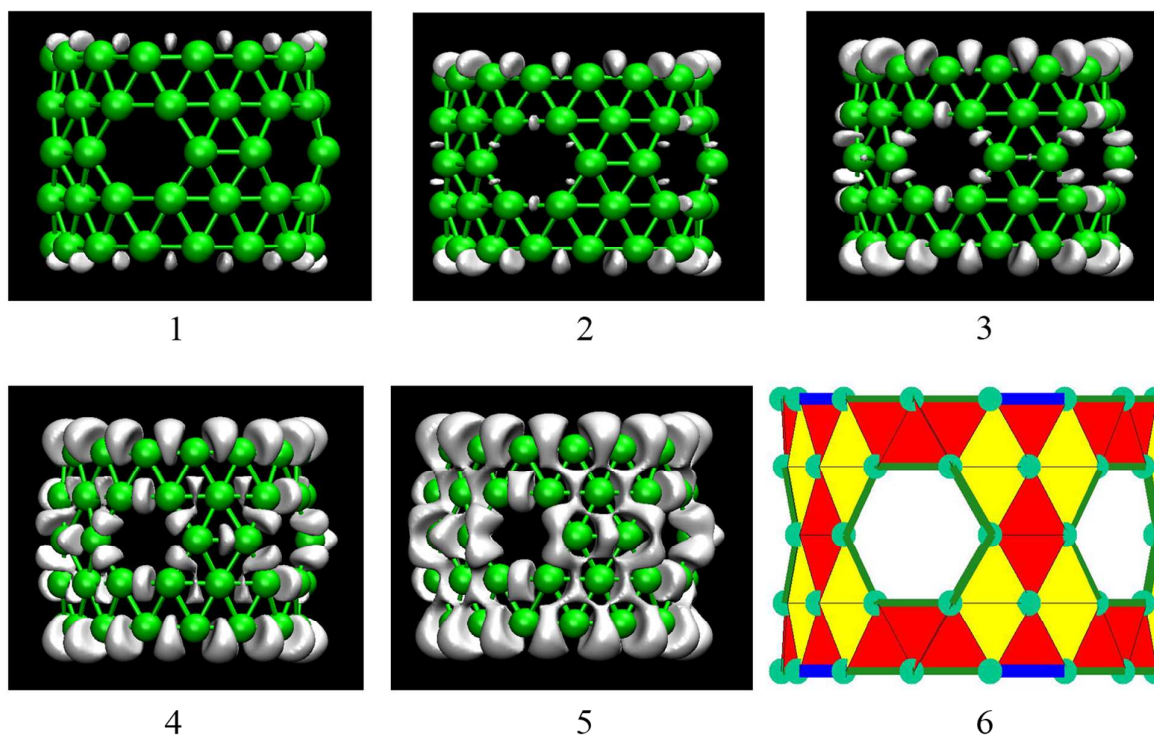

1

2

3

4

5

6

Figure S10. The ELF with different isosurface value and the bonding analysis for the tubular B_{70} cluster. The iso-value of (a-1~5) are 0.92, 0.89, 0.83, 0.78 and 0.74, respectively. (a-6) represents the distribution of 2c-2e and 3c-2e bonds.